Bond, R., Bryant, S., Watson, J., Hancox, J., Orchard, C., & James, A. (2017). Reduced density and altered regulation of rat atrial L-type Ca^{2+} current in heart failure. *AJP - Heart and Circulatory Physiology*, *312*(3), H384-H391. https://doi.org/10.1152/ajpheart.00528.2016

Reduced density and altered regulation of rat atrial L-type Ca^{2+} current in heart failure

First author & short title: Bond, Atrial L-type Ca^{2+} current in heart failure

Richard C. Bond, Simon M. Bryant, Judy J. Watson, Jules C. Hancox, Clive H. Orchard, Andrew F. James

Cardiovascular Research Laboratories, School of Physiology, Pharmacology & Neuroscience, University of Bristol, Bristol, United Kingdom

Author contributions

RCB: Whole-cell recordings, data analysis. SMB: Surgery for heart failure model. JJW: Western blot analysis. JCH: Involved in discussion and interpretation of data. CHO: Involved in inception of the project, discussion of the data. AFJ: Inception of the project, day-to-day supervision, discussion of the data, drafting manuscript. All authors contributed to writing of the manuscript

Word count: 7041 words (Abstract = 250 words)

Running Head: Atrial L-type Ca current in heart failure

Correspondence address: Dr Andrew F James, School of Physiology, Pharmacology & Neuroscience, Biomedical Sciences Building, University of Bristol, Bristol, BS8 1TD, United Kingdom. Tel. +44-(0)117-331-2297. Fax. +44-(0)117-331-2288. Email: a.james@bristol.ac.uk

Abstract

Constitutive regulation by PKA has recently been shown to contribute to L-type Ca^{2+} current (I_{CaL}) at the ventricular t-tubule in heart failure. Conversely, reduction in constitutive regulation by PKA has been proposed to underlie the downregulation of atrial I_{CaL} in heart failure. The hypothesis that downregulation of atrial I_{CaL} in heart failure involves reduced channel phosphorylation was examined. Anesthetized adult male Wistar rats underwent surgical coronary artery ligation (CAL, *N*=10) or equivalent sham-operation (Sham, *N*=12). Left atrial myocytes were isolated ~18 weeks post-surgery and whole-cell currents recorded (holding potential=-80 mV). I_{CaL} activated by depolarizing pulses to voltages from -40 to +50 mV were normalized to cell capacitance and current density-voltage relations plotted. CAL cell capacitances were ~1.67-fold greater than Sham (P≤0.0001). Maximal I_{CaL} conductance (G_{max}) was downregulated more than 2-fold in CAL vs Sham myocytes (P<0.0001). Norepinephrine (1 µmol/L) increased G_{max} >50% more effectively in CAL than in Sham so that differences in I_{CaL} density were abolished. Differences between CAL and Sham G_{max} were not abolished by calyculin A (100 nmol/L) , suggesting that increased protein dephosphorylation did not account for I_{CaL} downregulation. Treatment with either H-89 (10 µmol/L) or AIP (5 µmol/L) had no effect on basal currents in Sham or CAL myocytes, indicating that, in contrast to ventricular myocytes, neither PKA nor CaMKII regulated basal I_{CaL}. Expression of the L-type α_{1C}-subunit, protein phosphatases 1 and 2A and inhibitor-1 proteins was unchanged. In conclusion, reduction in PKA-dependent regulation did not contribute to downregulation of atrial I_{CaL} in heart failure.

Key words: atrial remodeling, coronary artery ligation, voltage-gated Ca^{2+} channel

New and Noteworthy Statement

Whole-cell recording of L-type Ca^{2+} currents in atrial myocytes from rat hearts subjected to coronary artery ligation in comparison with those from sham-operated controls reveals marked reduction in current density in heart failure without change in channel subunit expression and associated with altered phosphorylation independent of protein kinase A.

Introduction

Atrial fibrillation (AF) is the most common clinical arrhythmia and is associated with significant mortality, primarily through stroke and heart failure (2, 3). There are many causes of AF and although patients generally show multiple predisposing risk factors, >70% of patients have some form of underlying structural heart disease (2, 3). Evidence from animal models of heart diseases that predispose to AF indicates that disease-associated remodeling of the atria, presumably due to mechanical overload of the atrial wall, creates an arrhythmic substrate in which AF is more likely to arise and be sustained (10, 13, 22, 29, 30, 32, 34, 48). In addition to atrial enlargement, fibrosis and conduction abnormalities that establish a substrate for re-entry, cellular remodeling involving cellular hypertrophy, changes in membrane structure and abnormal expression and function of ion channels and transporters are also likely to contribute to the genesis of AF (4, 10, 13, 15, 16, 18, 22, 26, 29, 30, 32, 34, 35, 38, 48, 51).

Atrial L-type Ca^{2+} current (I_{CaL}) is reduced in heart disease, both in animal models (4, 13, 29, 38) and in myocytes from human dilated atria (19, 33). The loss of I_{CaL} has been suggested to have a number of sequelae that contribute to the genesis of AF, including (i) changes in action potential configuration and the rate-dependence of refractoriness, (ii) abnormalities in Ca^{2+} handling and the triggering of episodes of AF and (iii) hypo-contractility and dilatation of the atria (15, 29, 33, 35, 42). The mechanisms for the downregulation of I_{CaL} remain unclear and may be dependent on the underlying disease. For example, both spontaneously hypertensive rats and rats with coronary artery ligation-induced myocardial infarction show a substrate for atrial fibrillation associated with atrial fibrosis, hypertrophy and down-regulation in I_{CaL} (4, 10, 13, 38). However, while the reduced I_{CaL} density in atrial

myocytes from spontaneously hypertensive rats compared to currents in normotensive Wistar-Kyoto controls has been associated with reduction in expression of the pore-forming α_{1c} subunit, α_{1c} protein expression was unchanged in rat atrial myocytes from a coronary artery ligation model (4, 38). The reduction in atrial I_{CaL} in coronary artery ligation-induced heart failure has been suggested to be due to decreased cyclic AMP-dependent basal regulation of L-type Ca^{2+} channels (4, 19). However, while the cyclic AMP-dependent protein kinase, PKA, has also been demonstrated to play an important role in the basal regulation of I_{CaL} in ventricular myocytes (7, 8), the constitutive regulation of ventricular I_{CaL} by PKA appears to be increased in a coronary artery ligation model of heart failure (9). In addition, the reduction in atrial I_{CaL} in patients with chronic AF has been associated with a reduction in calcium-calmodulin-dependent protein kinase II (CaMKII) activity and an increase in protein phosphatase activity in AF with no change in the expression of L-type Ca^{2+} channel subunit protein (14). Changes in the activity of the serine/threonine protein phosphatases, PP1 and PP2A, and the regulatory subunit of PP1, inhibitor-1, have been implicated in the pro-arrhythmic remodeling in AF (25). Thus, the aim of this study was to examine the mechanisms underlying the regulation of atrial I_{CaL} in heart failure. The study involved the use of the coronary artery ligation model of myocardial infarction-associated heart failure reported previously (9, 23).

Materials & Methods

Animals, heart failure and myocyte isolation. All procedures were performed in accordance with UK legislation and approved by the University of Bristol Ethics Committee. The study was conducted in parallel with another investigation using the same animals to investigate ventricular cellular remodeling in heart failure and thereby conformed to the reduction component of the 3Rs (9, 23, 41). Heart failure was induced in 10 adult male Wistar rats by ligation of the left anterior descending coronary artery (CAL), which results in left ventricular hypertrophy and dilatation, and systolic and diastolic dysfunction 16 weeks after surgery (9, 36). 12 adult male Wistar rats were subject to an equivalent Sham operation (Sham). Left atrial myocytes were isolated ~18 weeks after surgery. Operations were performed under surgical anesthesia (ketamine 75 mg/kg, medetomidine 0.5 mg/kg, ip) with appropriate analgesia (buprenorphine 0.05 mg/kg, sc). We have previously reported that left ventricular ejection fraction was reduced by 50% and left ventricular end diastolic volume was increased by more than 100% in CAL as compared with Sham for this group of animals (9). Atrial myocytes were isolated using our standard methods (6, 8), following rapid excision of the heart under pentobarbitone anesthesia. Isolated myocytes were stored for 2-10 hours before use on the day of isolation.

Whole-cell recording. Whole-cell currents were recorded using the ruptured-patch technique, as described previously (6). Myocytes were superfused with Tyrode's solution comprising (mmol/L): 140 NaCl, 4 KCl, 1 $MgCl_2$, 2.5 $CaCl_2$, 10 D-glucose and 5 HEPES, pH 7.4 at 36 ^{o}C. The internal solution comprised (mmol/L): 10 NaCl, 110 KCl, 0.4 $MgCl_2$, 5 D-glucose, 10 HEPES, 5 BAPTA, 5 K-ATP and 0.5 Tris-GTP, pH 7.3 (KOH). Currents were low-pass filtered with a corner frequency of 1 kHz and recorded to the hard drive of a PC at a

sampling frequency of 5 kHz. The junction potential was compensated electronically on immersion of the pipette tip in the bath solution and no further compensation was applied. Whole-cell capacitance transients were compensated electronically. Series resistances were typically between 3 – 8 MΩ in both Sham and CAL myocytes and were not compensated and no corrections were made for voltage-drop error. A square-shaped voltage pulse protocol was applied: from a holding potential of -80 mV, 500 ms depolarizing pulses to potentials from -40 mV to +50 mV were applied, increasing in 10 mV increments every 5 s. A 50 ms pre-pulse to -40 mV was used to inactivate the Na^+ current. The L-type Ca^{2+} current (I_{CaL}) was measured as the difference between the peak inward current and the current at the end of the pulse. Although the inward currents recorded under these conditions could be completely abolished using 3 µmol/L nifedipine, the contribution of transient outward currents may have led to a slight under-estimation in I_{CaL} (13). Current densities were calculated as the currents normalized to whole-cell capacitance. Mean I_{CaL} values were plotted against the corresponding voltage and the current-voltage relation fitted by a modified Boltzmann equation:

$$I_{CaL}(V_m) = \frac{G_{max} \cdot (V_m - V_{rev})}{\left(1 + \exp\left(\frac{V_{half} - V_m}{k}\right)\right)}, \quad (1)$$

where V_m was the membrane potential, G_{max} represented the maximum conductance, V_{rev} was the effective reversal potential for the current, V_{half} represents the voltage of half-maximal activation and k represented a slope factor (6). Fitted parameters are reported with the standard error of fitting.

Drugs and reagents. All reagents were purchased from Sigma-Aldrich (Poole, UK) unless otherwise indicated. Norepinephrine (NE) was dissolved in de-ionized water as a 10 mmol/L stock-solution and dissolved to the final concentration in the extracellular solution on the day of experiment. 1 μmol/L of NE was used as an effective concentration of the physiological agonist of adrenoceptors previously shown to potentiate I_{CaL} maximally and that is representative of concentrations achieved at the cardiac sympathetic junction (6, 24). Protein kinase A (PKA) was inhibited using 10 μmol/L H-89, a concentration that has been shown to inhibit phosphorylation of the cardiac α_{1c} L-type Ca^{2+} channel subunit (12). In some experiments, autocamtide-2-related inhibitory peptide (AIP) was included in the pipette solution (5 μmol/L) to inhibit Ca^{2+}-calmodulin-dependent kinase II (CaMKII) (27). Calyculin A (Cal A) was used at a concentration of 100 nmol/L to inhibit the serine/threonine protein phosphatases 1 (PP1) and 2A (PP2A) (39).

Western blotting. 30 μg of protein from cell homogenate samples was run on reducing 4-15% gradient SDS-PAGE gels and transferred to Immobilon-P membranes. Membranes were probed with anti-$Ca_v1.2$ L-type Ca^{2+} channel α_{1c} subunit (ACC-003; Alomone, Israel), anti-protein phosphatase 1 (anti-PP1, sc-7482; Santa Cruz Biotechnology Inc., Texas, USA), anti-protein phosphatase 2A (anti-PP2A, 05-421; Millipore (UK) Ltd, Watford, UK) and anti-protein phosphatase inhibitor-1 (anti-Inhibitor-1, ab-40877; AbCam, Cambridge, UK). Protein bands were visualized and images captured using the appropriate horseradish peroxidase-conjugated secondary antibodies, chemiluminescence and a G:BOX Chemi XT4 imaging system (Syngene). The densities of the bands were measured using ImageJ (https://imagej.nih.gov/ij/) and normalized to the density of the GAPDH band (Sigma-Aldrich UK Ltd, Poole, UK).

Statistical analysis. Data are presented as the mean ± S.E.M. Statistical analyses were performed using Prism (vs5.04, GraphPad Software Inc., USA). Data sets were subject to D'Agostino-Pearson omnibus normality test. Sample sizes are provided in the Figure Legends as (*n* numbers of cells/*N* numbers of animals). Sham versus CAL comparisons in single parameters were analyzed using either Mann-Whitney or Student's unpaired *t*-test. Correlation analysis was performed using Spearman's rank correlation coefficient. Current-voltage relations were analyzed by two-way repeated measures (RM) ANOVA with Bonferroni *post hoc* test. Other results were analyzed by one-way RM ANOVA with Bonferroni's multiple-comparisons test. $P \leq 0.05$ was considered as the limit of statistical confidence.

Results

Single left atrial myocytes were isolated from Sham and CAL rats 18.9±0.45 weeks (*n*=12) and 18.7±0.48 weeks (*n*=10, P=0.678) following surgery, respectively. On the day of isolation, there was little difference between the two groups in body weight (Sham, 447.3±9.04 g vs CAL, 491.5±20.1 g; P=0.052) or tibia length (Fig. 1A). However, CAL animals showed significantly increased heart weights (HW) and lung weights (LW) relative to tibia length (TL; Fig. 1B), indicative of early stage heart failure as demonstrated in our previous report using these hearts (9). In summary, the data indicate early onset heart failure in the CAL animals in the present study. Whole-cell capacitance values of left atrial myocytes isolated from CAL hearts were ~1.67 times larger than those from Sham controls, indicating considerable cellular hypertrophy of atrial myocytes in heart failure (Fig. 2A). Cell length and width were measured in 12 Sham (from 2 hearts) and 12 CAL (from 2 hearts) isolated atrial myocytes. While there was no difference in cell length (Sham 103.6±4.1 μm, CAL 113.1±5.8 μm; P=0.1938), cell width was significantly greater in CAL compared with Sham myocytes (Sham 14.5±1.0 μm, CAL 22.0±1.3 μm; P=0.0001). Taken together, these data are consistent with the atrial hypertrophy previously reported in coronary artery ligation models of heart failure (10, 50).

Figure 2B shows representative recordings from Sham and CAL myocytes of L-type Ca^{2+} current (I_{CaL}) elicited by depolarizing pulses to +10 mV. Mean I_{CaL}-voltage relations in Sham and CAL myocytes are shown in Figure 2C. In both groups of cells, currents were activated from voltages of -30 mV, were maximal at around +10 mV and reversed at ~+50 mV, typical of cardiac I_{CaL} (Fig. 2C). I_{CaL}-voltage relations were fitted with a modified Boltzmann equation (equation 1; see Methods). There were no differences between CAL and Sham myocytes in

the voltage of half-maximal activation (V_{half}: Sham -0.72±1.5 mV, CAL: -1.09±2.46 mV), slope factor (k: Sham 6.89±0.86 mV, CAL 6.11±1.51 mV) or reversal potential (V_{rev}: Sham 48.25±1.38 mV, CAL 49.83±2.94 mV), indicating no significant changes in the voltage-dependence or ion selectivity of I_{CaL} in heart failure. However, while the differences between CAL and Sham myocytes in mean I_{CaL} did not reach statistical confidence at any potential, the fitted maximal conductance was less in CAL than in Sham cells (G_{max}: Sham 17.01±1.51 nS, CAL 11.66±1.92 nS; P=0.0317). After normalization to cell capacitance, the corresponding mean current density-voltage relations (Fig. 2D) show significantly smaller I_{CaL} density in CAL myocytes compared to Sham controls at voltages from -10 to +30 mV. The maximal conductance density was reduced by more than 50% in CAL compared to Sham myocytes (G_{max}: Sham 288.4±24.2 pS/pF, CAL 140.6±16.5 pS/pF; P<0.0001). The correlation between I_{CaL} density at +10 mV and cell capacitance in atrial cells from Sham and CAL hearts is shown in Figure 2E. In CAL cells, I_{CaL} density was inversely correlated with capacitance (r=-0.4219, n=31, P=0.0181). Taken together, these data indicate that heart failure through coronary artery ligation causes a reduction in whole-cell I_{CaL} density of left atrial myocytes that is predominantly due to an increase in cell membrane surface area with minor changes in absolute current.

The reduction in atrial I_{CaL} density by more than 50% caused by CAL-induced heart failure was consistent with a previous report in a similar model, in which it was also shown that the difference in I_{CaL} density between sham control and heart failure was reduced following β-adrenoceptor stimulation with isoproterenol (4). The sympathetic neurotransmitter, NE, has previously been shown to potentiate atrial I_{CaL} via β_1-adrenoceptors without significant contribution from either α_1- or β_2-adrenoceptors (6). Therefore, the effects of NE on

differences in I_{CaL} density between Sham and CAL atrial myocytes were examined. As illustrated by the representative current traces in Figure 3, 1 μmol/L NE produced a marked increase in I_{CaL} in both Sham and CAL myocytes (Fig. 3A & Fig. 3B). Notably, although statistically significant differences in I_{CaL} density-voltage relations (Fig. 3C) and maximal conductance density were evident under control conditions (G_{max}: Sham 371.6±65.2 pS/pF, CAL 182.0±28.6, P=0.0091), these differences were lost in the presence of NE (Fig. 3D; G_{max}: Sham 660.6±113.2 pS/pF, CAL 494.3±61.2 pS/pF, P=0.1798). Thus, NE had a greater effect on G_{max} in CAL (2.72-fold increase) than in Sham (1.78-fold increase) myocytes. In addition, V_{half} was negatively shifted by NE in both cell types (Sham control 1.85±2.98 mV to NE -4.38±2.43 mV, P=0.1434; CAL control 2.93±2.50 mV to NE -5.57±1.66 mV, P=0.0121). Overall, these data demonstrate differences in the regulation of the L-type Ca^{2+} channel currents between Sham and CAL cells. To examine whether constitutive phosphorylation of LTCC contributed to the differences in I_{CaL} density, cells were superfused with the serine/threonine protein phosphatase inhibitor, calyculin A (100 nmol/L) (Fig. 4). In both groups of cells, calyculin A resulted in increased mean current densities at voltages from -20 mV to +40 mV (Fig. 4). However, the relative increase in maximal conductance was not significantly different between the two groups (P=0.4850): in Sham cells, G_{max} was increased 2.75-fold (control 187.2±26.9 pS/pF, calyculin A 514.5±47.4 pS/pF, P<0.0001), whereas in CAL cells G_{max} was increased 3.34-fold (control 111.3±14.2 pS/pF, calyculin A 371.7±36.1 pS/pF, P<0.0001). Critically, in contrast to the effect of NE, in the presence of calyculin A, G_{max} was greater in Sham than in CAL cells (two-way ANOVA, Bonferroni post hoc test, P<0.01).

The role of protein kinase A in differences in basal I_{CaL} density between the two groups of atrial cells was examined using the PKA inhibitor, H-89 (10 µmol/L) (Fig. 5). Superfusion of cells with H-89 had no effect on basal I_{CaL} in either Sham (Fig. 5A) or CAL (Fig. 5B) myocytes, although the response to NE (1 µmol/L) was abolished. Further evidence that PKA does not contribute to the constitutive regulation of I_{CaL} was obtained in a small series of experiments conducted in Sham cells only, in which the increase in I_{CaL} density on superfusion with 100 nmol/L calyculin A was not abolished by application of the PKA inhibitor, PKI (20 µmol/L), via the pipette solution (data not shown). CaMKII has also been suggested to contribute to basal I_{CaL} in atrial myocytes (17). Therefore, we examined the effect on basal I_{CaL} of inhibition of CaMKII with AIP (5 µmol/L) applied via the intracellular pipette solution in Sham and CAL cells (Figure 6). Comparison of the mean current density-voltage relations of the Sham (Fig. 6A) and CAL (Fig. 6B) myocytes dialyzed with AIP (filled symbols in the figure) with the corresponding control data (gray-filled symbols) showed no effect of AIP on basal I_{CaL} in either cell type. Moreover, I_{CaL} density was increased by 100 nmol/L calyculin A in both Sham and CAL cells dialyzed with AIP. Further evidence that CaMKII played no role in basal I_{CaL} came from a small number of experiments in which Sham myocytes were superfused with the CaMKII inhibitor, KN-93 (5 µmol/L). Treatment with KN-93 had no effect on mean I_{CaL} density at +10 mV in Sham cells (data not shown). Taken together, these data suggest that inhibition of CaMKII had no effect on basal I_{CaL} in either Sham or CAL myocytes.

The expression of proteins for the predominant LTCC pore-forming α_{1c} subunit, $Ca_v1.2$, for the serine/threonine protein phosphatases, PP1 and PP2A, and for the inhibitory subunit of PP1, inhibitor-1, was examined by Western blotting in atrial cell preparations from 3 Sham and 3 CAL hearts (Figure 7). There were no significant differences in the total content of α_{1c}

subunit relative to GAPDH expression between the two groups of cells. The increase in I_{CaL} density on inhibition of protein phosphatase with calyculin A (Fig. 4) indicates a role for protein phosphorylation in the basal regulation of L-type Ca^{2+} channels in both groups of cells. However, expression of neither PP1 nor PP2A were changed in heart failure (Fig. 7). Moreover, the PKA-dependent inhibitory regulator of PP1, inhibitor-1, reduced expression of which in failing ventricles has been suggested to contribute to reduced protein phosphorylation (20), was also not different between the two groups of cells.

Discussion

This study clearly demonstrates a reduction in atrial I_{CaL} density in heart failure, due predominantly to cellular hypertrophy without significant change in absolute current amplitude. However, the total expression of the α_{1c} subunit protein relative to total tissue protein was also not changed in heart failure, indicating that the reduction in basal current density in heart failure did not involve significant changes in the relative amount of protein in hypertrophied cells. It seems likely that a change in L-type Ca^{2+} channel regulation underlay the reduction in I_{CaL} density. The difference in I_{CaL} density between atrial cells from failing and sham hearts was abolished in the presence of NE, which increased the L-type Ca^{2+} current >50% more effectively in CAL cells than in Sham. Moreover, the increase in current density produced by inhibition of serine/threonine protein phosphatase activity with calyculin A provides evidence of phosphorylation-dependent basal regulation of I_{CaL} in both groups of cells. In these respects, the data resemble those reported by Dinanian *et al* in human atrial myocytes from patients with heart failure (19) and by Boixel *et al* in a model of coronary artery ligation-induced heart failure in rats similar to that used in the present study (4) and contrast with studies of chronic hypertension and pressure overload in rats that show a reduction in atrial α_{1c} subunit protein expression (38, 51). However, contrary to the mechanism proposed by Boixel *et al*. (4), the insensitivity of basal I_{CaL} to H-89 and PKI in the present study demonstrated that protein kinase A did not contribute to the constitutive regulation of atrial I_{CaL}. This finding differs from the conclusion of Boixel *et al* that the downregulation of atrial I_{CaL} in heart failure was "*… caused by changes in basal cAMP-dependent regulation of the current …*" (4). A notable difference between that study and this is that Boixel *et al* did not report the effects of inhibition of protein kinase A (4).

Basal I_{CaL} in the present study was also insensitive to AIP and KN-93, demonstrating that, unlike human atrial myocytes, CaMKII did not contribute to the constitutive regulation of the L-type Ca^{2+} current (14).

The present study showed little difference between atrial cells from failing hearts and sham controls in the effectiveness of inhibition of the protein phosphatases PP1 and PP2A so that, in contrast to previous reports, differences in protein dephosphorylation via these phosphatases are unlikely to account for the downregulation of atrial I_{CaL} density in heart failure (4, 14). Consistent with this suggestion, no differences were found in the expression of PP1, PP2A or inhibitor-1. The basis for the differences between the study of Boixel *et al* and the present study, in which similar models of heart failure were used, remain unclear although it is possible that the results of the present study, in which animals were maintained for 18 weeks following coronary artery ligation, represent a more chronic state of remodeling than did those of Boixel *et al*, in which animals were maintained for 3 months post-surgery (4, 9, 36, 37).

The mechanism for the down regulation of atrial I_{CaL} in heart failure remains unclear. A number of kinases, including PKC, PKD, PKG and tyrosine kinases, have been reported to modulate cardiac I_{CaL} and, in principle, changes in the activity of any of these could contribute to the reduction in basal I_{CaL} in heart failure (1, 5, 28). Additionally, calcineurin (PP2B) has been suggested to associate with and regulate the L-type Ca^{2+} channel α_{1c}-subunit and to contribute to down-regulation of I_{CaL} during atrial remodeling (46, 53). Atrial I_{CaL} is also regulated by NO through complex pathways involving cyclic GMP-dependent PKG, cyclic GMP-inhibited phosphodiesterases, and S-nitrosylation of the α_{1c}-subunit (31, 40, 47, 49). It has been suggested that oxidative stress may contribute to the development of the

arrhythmic substrate and down-regulation of I_{CaL} during atrial remodeling and this may involve changes in the NO-dependent regulation of L-type Ca^{2+} channels (11, 21, 43). The previously reported changes in atrial intracellular cyclic GMP production together with the increased effect of phosphodiesterase inhibition on I_{CaL} are consistent with the proposal that changes in NO/cGMP-dependent regulation of L-type Ca^{2+} channels may underlie both the reduced basal current and increased sensitivity to noradrenergic agonism in heart failure (4, 19). On the other hand, while it has previously been shown that the effect of NE on I_{CaL} is almost exclusively mediated via β_1-adrenoceptors in atrial myocytes from normal hearts (6), the contribution of α_1-, β_2 and β_3-adrenoceptors in heart failure cannot be ruled out (44, 45, 52). Thus, future studies using selective adrenoceptor ligands and inhibitors of signaling cascades will be important to establish the mechanism underlying the remodeling of atrial I_{CaL} regulation in heart failure.

The present study also adds to evidence that the mechanisms of I_{CaL} regulation differ between atrial and ventricular cells (6-8). While both PKA and CaMKII have previously been shown to contribute to the basal regulation of ventricular I_{CaL}, particularly at the t-tubule membrane, (7-9, 12), basal I_{CaL} in atrial myocytes from either sham control or failing hearts in the present study was insensitive to inhibition of PKA or CaMKII. Notably, the absence of regulation of basal atrial I_{CaL} by PKA in CAL hearts in the present study contrasts markedly with the increased PKA-dependent regulation of basal I_{CaL} at the t-tubule of ventricular myocytes reported recently from the same hearts (9). The action of calyculin A on atrial I_{CaL} demonstrates both that the basal regulation of I_{CaL} in rat atrial myocytes depends on constitutive phosphorylation by a serine/threonine kinase and that PP1/PP2A phosphatase activity contributes to the degree of basal phosphorylation. Thus, the identity of the kinases

and phosphatases responsible for the constitutive regulation of atrial I_{CaL} in both normal hearts and in heart failure warrants further investigation.

Acknowledgements

We thank Marcus Sikkel (Imperial College, London) for advice and guidance in establishing the coronary artery ligation model of heart failure.

Funding Sources

This work was supported by the *British Heart Foundation* (FS/10/68 to RB, PG/10/91 to CHO and AFJ and PG/11/97 to JCH and AFJ).

Disclosures

RB was in receipt of a fellowship from the *British Heart Foundation* that funded this work (FS/10/68). AFJ and JCH were lead applicants on the fellowship that funded this work (FS/10/68). CHO and AFJ were principal investigators on the project and programme grants that funded SMB (PG/10/91, RG/12/10).

References

1. **Aita Y, Kurebayashi N, Hirose S, and Maturana AD**. Protein kinase D regulates the human cardiac L-type voltage-gated calcium channel through serine 1884. *FEBS Lett* 585: 3903-3906, 2011.
2. **Andrade J, Khairy P, Dobrev D, and Nattel S**. The Clinical Profile and Pathophysiology of Atrial Fibrillation: Relationships Among Clinical Features, Epidemiology, and Mechanisms. *Circ Res* 114: 1453-1468, 2014.
3. **Benjamin EJ, Chen P-S, Bild DE, Mascette AM, Albert CM, Alonso A, Calkins H, Connolly SJ, Curtis AB, Darbar D, Ellinor PT, Go AS, Goldschlager NF, Heckbert SR, Jalife J, Kerr CR, Levy D, Lloyd-Jones DM, Massie BM, Nattel S, Olgin JE, Packer DL, Po SS, Tsang TSM, Van Wagoner DR, Waldo AL, and Wyse DG**. Prevention of Atrial Fibrillation: Report From a National Heart, Lung, and Blood Institute Workshop. *Circulation* 119: 606-618, 2009.
4. **Boixel C, Gonzalez W, Louedec L, and Hatem SN**. Mechanisms of L-Type Ca^{2+} Current Downregulation in Rat Atrial Myocytes During Heart Failure. *Circ Res* 89: 607-613, 2001.
5. **Boixel C, Tessier S, Pansard Y, Lang-Lazdunski L, Mercadier J-J, and Hatem SN**. Tyrosine kinase and protein kinase C regulate L-type Ca^{2+} current cooperatively in human atrial myocytes. *Am J Physiol* 278: H670-676, 2000.
6. **Bond RC, Choisy SCM, Bryant SM, Hancox JC, and James AF**. Inhibition of a TREK-like K^+ channel current by noradrenaline requires both β_1- and β_2-adrenoceptors in rat atrial myocytes. *Cardiovasc Res* 104: 206-215, 2014.
7. **Bracken N, ElKadri M, Hart G, and Hussain M**. The role of constitutive PKA-mediated phosphorylation in the regulation of basal I_{Ca} in isolated rat cardiac myocytes. *Br J Pharmacol* 148: 1108-1115, 2006.
8. **Bryant S, Kimura TE, Kong CHT, Watson JJ, Chase A, Suleiman MS, James AF, and Orchard CH**. Stimulation of I_{Ca} by basal PKA activity is facilitated by caveolin-3 in cardiac ventricular myocytes. *J Mol Cell Cardiol* 68: 47-55, 2014.
9. **Bryant SM, Kong CHT, Watson J, Cannell MB, James AF, and Orchard CH**. Altered distribution of I_{Ca} impairs Ca release at the t-tubules of ventricular myocytes from failing hearts. *J Mol Cell Cardiol* 86: 23-31, 2015.
10. **Cardin S, Guasch E, Luo X, Naud P, Le Quang K, Shi Y, Tardif J-C, Comtois P, and Nattel S**. A Role for MicroRNA-21 in Atrial Profibrillatory Fibrotic Remodeling Associated with Experimental Post-infarction Heart Failure. *Circ Arrhythm Electrophysiol* 5: 1027-1035, 2012.
11. **Carnes CA, Janssen PML, Ruehr ML, Nakayama H, Nakayama T, Haase H, Bauer JA, Chung MK, Fearon IM, Gillinov AM, Hamlin RL, and Van Wagoner DR**. Atrial Glutathione Content, Calcium Current, and Contractility. *J Biol Chem* 282: 28063-28073, 2007.
12. **Chase A, Colyer J, and Orchard CH**. Localised Ca channel phosphorylation modulates the distribution of L-type Ca current in cardiac myocytes. *J Mol Cell Cardiol* 49: 121-131, 2010.
13. **Choisy SCM, Arberry LA, Hancox JC, and James AF**. Increased Susceptibility to Atrial Tachyarrhythmia in Spontaneously Hypertensive Rat Hearts. *Hypertension* 49: 498-505, 2007.
14. **Christ T, Boknik P, Wohrl S, Wettwer E, Graf EM, Bosch RF, Knaut M, Schmitz W, Ravens U, and Dobrev D**. L-Type Ca^{2+} Current Downregulation in Chronic Human Atrial Fibrillation Is Associated With Increased Activity of Protein Phosphatases. *Circulation* 110: 2651-2657, 2004.
15. **Clarke JD, Caldwell JL, Horn MA, Bode EF, Richards MA, Hall MCS, Graham HK, Briston SJ, Greensmith DJ, Eisner DA, Dibb KM, and Trafford AW**. Perturbed atrial calcium handling in an ovine model of heart failure: Potential roles for reductions in the L-type calcium current. *J Mol Cell Cardiol* 79: 169-179, 2015.
16. **Climent AM, Guillem MS, Fuentes L, Lee P, Bollensdorff C, Fernández-Santos ME, Suárez-Sancho S, Sanz-Ruiz R, Sánchez PL, Atienza F, and Fernández-Avilés F**. Role of atrial tissue remodeling on rotor dynamics: an *in vitro* study. *Am J Physiol* 309: H1964-H1973, 2015.

17. **Collins TP, and Terrar DA**. Ca^{2+}-stimulated adenylyl cyclases regulate the L-type Ca^{2+} current in guinea-pig atrial myocytes. *J Physiol (Lond)* 590: 1881-1893, 2012.
18. **Dibb KM, Clarke JD, Horn MA, Richards MA, Graham HK, Eisner DA, and Trafford AW**. Characterization of an Extensive Transverse Tubular Network in Sheep Atrial Myocytes and its Depletion in Heart Failure. *Circ Heart Fail* 2: 482-489, 2009.
19. **Dinanian S, Boixel C, Juin C, Hulot J-S, Coulombe A, Rücker-Martin C, Bonnet N, Le Grand B, Slama M, Mercadier J-J, and Hatem SN**. Downregulation of the calcium current in human right atrial myocytes from patients in sinus rhythm but with a high risk of atrial fibrillation. *Eur Heart J* 29: 1190-1197, 2008.
20. **El-Armouche A, Pamminger T, Ditz D, Zolk O, and Eschenhagen T**. Decreased protein and phosphorylation level of the protein phosphatase inhibitor-1 in failing human hearts. *Cardiovasc Res* 61: 87-93, 2004.
21. **Emelyanova L, Ashary Z, Cosic M, Negmadjanov U, Ross G, Rizvi F, Olet S, Kress D, Sra J, Tajik AJ, Holmuhamedov EL, Shi Y, and Jahangir A**. Selective downregulation of mitochondrial electron transport chain activity and increased oxidative stress in human atrial fibrillation. *Am J Physiol* 311: H54-H63, 2016.
22. **Everett IV TH, Wilson EE, Verheule S, Guerra JM, Foreman S, and Olgin JE**. Structural atrial remodeling alters the substrate and spatiotemporal organization of atrial fibrillation: a comparison in canine models of structural and electrical atrial remodeling. *Am J Physiol* 291: H2911-H2923, 2006.
23. **Gadeberg HC, Bryant SM, James AF, and Orchard CH**. Altered Na/Ca exchange distribution and activity in ventricular myocytes from failing hearts. *Am J Physiol* 310: H262-H268, 2016.
24. **Goldstein DS, McCarty R, Polinsky RJ, and Kopin IJ**. Relationship between plasma norepinephrine and sympathetic neural activity. *Hypertension* 5: 552-559, 1983.
25. **Greiser M, Lederer WJ, and Schotten U**. Alterations of atrial Ca^{2+} handling as cause and consequence of atrial fibrillation. *Cardiovasc Res* 89: 722-733, 2011.
26. **Hohendanner F, DeSantiago J, Heinzel FR, and Blatter LA**. Dyssynchronous calcium removal in heart failure-induced atrial remodeling. *Am J Physiol Heart Circ Physiol* doi:10.1152/ajpheart.00375.2016.
27. **Ishida A, Kameshita I, Okuno S, Kitani T, and Fujisawa H**. A Novel Highly Specific and Potent Inhibitor of Calmodulin-Dependent Protein Kinase II. *Biochem Biophys Res Comm* 212: 806-812, 1995.
28. **Keef KD, Hume JR, and Zhong J**. Regulation of cardiac and smooth muscle Ca^{2+} channels (CaV1.2a,b) by protein kinases. *Am J Physiol* 281: C1743-C1756, 2001.
29. **Kettlewell S, Burton FL, Smith GL, and Workman AJ**. Chronic myocardial infarction promotes atrial action potential alternans, afterdepolarisations and fibrillation. *Cardiovasc Res* 99: 215-224, 2013.
30. **Kim S-J, Choisy SCM, Barman P, Zhang H, Hancox JC, Jones SA, and James AF**. Atrial Remodeling and the Substrate for Atrial Fibrillation in Rat Hearts with Elevated Afterload. *Circ Arrhythm Electrophysiol* 4: 761-769, 2011.
31. **Kirstein M, Rivet-Bastide M, Hatem S, Benardeau A, Mercadier J-J, and Fischmeister R**. Nitric oxide regulates the calcium current in isolated human atrial myocytes. *J Clin Invest* 95: 794-802, 1995.
32. **Kistler PM, Sanders P, Dodic M, Spence SJ, Samuel CS, Zhao C, Charles JA, Edwards GA, and Kalman JM**. Atrial electrical and structural abnormalities in an ovine model of chronic blood pressure elevation after prenatal corticosteroid exposure: implications for development of atrial fibrillation. *Eur Heart J* 27: 3045-3056, 2006.
33. **Le Grand B, Hatem S, Deroubaix E, Couetil J-P, and Coraboeuf E**. Depressed transient outward and calcium currents in dilated human atria. *Cardiovasc Res* 28: 548-556, 1994.
34. **Li D, Fareh S, Leung TK, and Nattel S**. Promotion of Atrial Fibrillation by Heart Failure in Dogs: Atrial Remodeling of a Different Sort. *Circulation* 100: 87-95, 1999.

35. **Li D, Melnyk P, Feng J, Wang Z, Petrecca K, Shrier A, and Nattel S**. Effects of Experimental Heart Failure on Atrial Cellular and Ionic Electrophysiology. *Circulation* 101: 2631-2638, 2000.
36. **Lyon AR, MacLeod KT, Zhang Y, Garcia E, Kanda GK, Lab MJ, Korchev YE, Harding SE, and Gorelik J**. Loss of T-tubules and other changes to surface topography in ventricular myocytes from failing human and rat heart. *Proc Natl Acad Sci USA* 106: 6854-6859, 2009.
37. **Michel JB, Lattion AL, Salzmann JL, Cerol ML, Philippe M, Camilleri JP, and Corvol P**. Hormonal and cardiac effects of converting enzyme inhibition in rat myocardial infarction. *Circ Res* 62: 641-650, 1988.
38. **Pluteanu F, Heß J, Plackic J, Nikonova Y, Preisenberger J, Bukowska A, Schotten U, Rinne A, Kienitz M-C, Schäfer MK-H, Weihe E, Goette A, and Kockskämper J**. Early subcellular Ca^{2+} remodeling and increased propensity for Ca^{2+} alternans in left atrial myocytes from hypertensive rats. *Cardiovasc Res* 106: 87-97, 2015.
39. **Resjo S, Oknianska A, Zolnierowicz S, Manganiello V, and Degerman E**. Phosphorylation and activation of phosphodiesterase type 3B (PDE3B) in adipocytes in response to serine/threonine phosphatase inhibitors: deactivation of PDE3B in vitro by protein phosphatase type 2A. *Biochem J* 341: 839–845, 1999.
40. **Rozmaritsa N, Christ T, Van Wagoner DR, Haase H, Stasch J-P, Matschke K, and Ravens U**. Attenuated response of L-type calcium current to nitric oxide in atrial fibrillation. *Cardiovasc Res* 101: 533-542, 2014.
41. **Russell WMS, and Burch RL**. *The Principles of Humane Experimental Technique*. Methuen, 1959.
42. **Schotten U, de Haan S, Neuberger H-R, Eijsbouts S, Blaauw Y, Tieleman R, and Allessie M**. Loss of atrial contractility is primary cause of atrial dilatation during first days of atrial fibrillation. *Am J Physiol* 287: H2324-H2331, 2004.
43. **Simon JN, Ziberna K, and Casadei B**. Compromised redox homeostasis, altered nitroso–redox balance, and therapeutic possibilities in atrial fibrillation. *Cardiovasc Res* 109: 510, 2016.
44. **Skeberdis VA, Jurevičius J, Fischmeister, and Rodolphe**. Beta-2 Adrenergic Activation of L-Type Ca^{++} Current in Cardiac Myocytes. *J Pharmacol Exp Therap* 283: 452-461, 1997.
45. **Steinfath M, Lavicky J, Schmitz W, Scholz H, Döring V, and Kalmár P**. Regional distribution of β_1- and β_2-adrenoceptors in the failing and nonfailing human heart. *Eur J Clin Pharmacol* 42: 607-611, 1992.
46. **Tandan S, Wang Y, Wang TT, Jiang N, Hall DD, Hell JW, Luo X, Rothermel BA, and Hill JA**. Physical and Functional Interaction Between Calcineurin and the Cardiac L-Type Ca^{2+} Channel. *Circ Res* 105: 51-60, 2009.
47. **Vandecasteele G, Verde I, Rucker-Martin C, Donzeau-Gouge P, and Fischmeister R**. Cyclic GMP regulation of the L-type Ca^{2+} channel current in human atrial myocytes. *J Physiol (Lond)* 533: 329-340, 2001.
48. **Verheule S, Wilson E, Banthia S, Everett TH, IV, Shanbhag S, Sih HJ, and Olgin J**. Direction-dependent conduction abnormalities in a canine model of atrial fibrillation due to chronic atrial dilatation. *Am J Physiol* 287: H634-H644, 2004.
49. **Wang Y-g, Wagner MB, Joyner RW, and Kumar R**. cGMP-dependent protein kinase mediates stimulation of L-type calcium current by cGMP in rabbit atrial cells. *Cardiovasc Res* 48: 310, 2000.
50. **Yoon N, Cho JG, Kim KH, Park KH, Sim DS, Yoon HJ, Hong YJ, Park HW, Kim JH, Ahn Y, Jeong MH, and Park JC**. Beneficial effects of an angiotensin-II receptor blocker on structural atrial reverse-remodeling in a rat model of ischemic heart failure. *Exp Ther Med* 5: 1009–1016, 2013.
51. **Zhang H, Cannell MB, Kim SJ, Watson JJ, Norman R, Calaghan SC, Orchard CH, and James AF**. Cellular Hypertrophy and Increased Susceptibility to Spontaneous Calcium-Release of Rat Left Atrial Myocytes Due to Elevated Afterload. *PLoS ONE* 10: e0144309, 2015.
52. **Zhang Z-S, Cheng H-J, Onishi K, Ohte N, Wannenburg T, and Cheng C-P**. Enhanced Inhibition of L-type Ca^{2+} Current by β_3-Adrenergic Stimulation in Failing Rat Heart. *J Pharmacol Exptl Therap* 315: 1203-1211, 2005.

53. **Zhao F, Zhang S, Chen L, Wu Y, Qin J, Shao Y, Wang X, and Chen Y**. Calcium- and integrin-binding protein-1 and calcineurin are upregulated in the right atrial myocardium of patients with atrial fibrillation. *Europace* 14: 1726-1733, 2012.

Figure Legends

Fig. 1. Atrial L-type Ca^{2+} current density in heart failure. A: Mean tibia length from 12 Sham and 10 CAL rats. *, P<0.05; Mann-Whitney test. B: Mean heart weight/tibia length and lung weight/tibia length ratios. Sham, filled columns and CAL, open columns. **, P<0.01; ****, P<0.001; Mann-Whitney test.

Fig. 2. A: Whole-cell capacitances for Sham (*n*=63/12) and CAL (*n*=47/10) myocytes. ****, P<0.0001; Mann-Whitney test. B: Representative whole-cell L-type Ca^{2+} current (I_{CaL}) traces at +10 mV. Sham: black. CAL: gray. C: Mean I_{CaL}-voltage relations for Sham (filled circles, *n*=32/12) and CAL (open circles, *n*=31/10) myocytes. D: Mean I_{CaL} density-voltage relations for Sham (filled circles) and CAL (open circles) myocytes. The same data as shown in C. **, P<0.01; ***, P<0.001; two-way RM ANOVA with Bonferroni post-test. Solid lines in C and D represent fits to equation 1. E: Correlation between I_{CaL} density at +10 mV in Sham (filled circles, *n*=32/12) and CAL (open circles, *n*=31/10) myocytes. Atrial I_{CaL} density for the two groups of cells combined was significantly correlated (r=-0.4772, *n*=63/22, P<0.0001).

Fig. 3. Effects of norepinephrine on atrial L-type Ca^{2+} current (I_{CaL}) density. A: Representative Ca^{2+} current traces at +10 mV in an atrial myocyte from a Sham-operated rat in control conditions and in the presence of 1 µmol/L norepinephrine. B: Representative Ca^{2+} current traces in an atrial myocyte from a CAL rat in control conditions and in the presence of 1 µmol/L norepinephrine. Arrows indicate zero current level. C: Mean I_{CaL} density-voltage relations under control conditions from

Sham-operated (*n*=5/3, filled circles) and CAL (*n*=9/4, open circles). *, P<0.05, Bonferroni post-test following two-way RM ANOVA. D: Mean I_{CaL} density-voltage relations in the presence of 1 µmol/L norepinephrine from Sham-operated (*n*=5/3, open squares) and CAL (*n*=9/4, filled squares). Data correspond to the control data shown in (C). Note the difference in current density scale between panels C and D. Solid lines in panels C and D represent fits to equation 1.

Fig. 4. Atrial L-type Ca^{2+} currents following phosphatase inhibition. A: (i) Representative current traces recorded at +10 mV from a Sham myocyte before and after superfusion with 100 nmol/L calyculin A. (ii) I_{CaL} density-voltage relations from Sham myocytes (*n*=6/3) in control (filled circles) and in the presence of 100 nmol/L calyculin A (open circles). *, P<0.05; ***, P<0.001; two-way RM ANOVA and Bonferroni post-test. B: (i) Representative current traces recorded at +10 mV from a CAL myocyte before and after superfusion with 100 nmol/L calyculin A. (ii) I_{CaL} density-voltage relations from CAL myocytes (*n*=9/3) in control (filled squares) and in the presence of 100 nmol/L calyculin A (open squares). ***, P<0.001; two-way ANOVA and Bonferroni post-test.

Fig. 5. Effect of the protein kinase A inhibitor, H-89. A: (i) Representative Ca^{2+} current traces at +10 mV in an atrial myocyte from a Sham-operated rat in control Tyrode's, in the presence of 10 µmol/L H-89 and in the presence of 10 µmol/L H-89 and 1 µmol/L norepinephrine (NE). (ii) Mean I_{CaL} density-voltage relations from Sham myocytes (*n*=8/4) in control (filled circles), in the presence of 10 µmol/L H-89 (gray-filled circles) and in the presence of 10 µmol/L H-89 and 1 µmol/L NE (open circles). B: (i)

Representative Ca^{2+} current traces in an atrial myocyte from a CAL rat in control Tyrode's, in the presence of 10 µmol/L H-89 and in the presence of 10 µmol/L H-89 and 1 µmol/L NE. Right-pointing arrows indicate zero current level. (ii) Mean I_{CaL} density-voltage relations from CAL myocytes (*n*=13/4) in control (filled squares), in the presence of 10 µmol/L H-89 (gray-filled squares) and in the presence of 10 µmol/L H-89 and 1 µmol/L NE (open squares).

Fig. 6. Effect of the Ca^{2+}-calmodulin-dependent protein kinase II inhibitor, AIP. A: Mean I_{CaL} density-voltage relations for Sham myocytes with AIP included in the pipette solution (*n*/*N*=4/1). Filled circles – AIP-dialyzed cells in control Tyrode's, open circles – AIP-dialyzed cells in the presence of 100 nmol/L calyculin A. B: Mean I_{CaL} density-voltage relations for CAL myocytes with AIP included in the pipette solution (*n*/*N*=5/1). Filled squares – AIP-dialyzed cells in control Tyrode's, open squares – AIP-dialyzed cells in the presence of 100 nmol/L calyculin A. Data from Sham (A) and CAL (B) myocytes under control conditions (respectively, *n*=33/12 and 31/10) are shown as, respectively, gray-filled circles and gray-filled squares, for comparison. **, P<0.01; ***, P<0.001; two-way RM ANOVA and Bonferroni post-test vs corresponding AIP control.

Fig. 7. Left atrial expression of the $Ca_v1.2$ LTCC α_{1c} subunit and various protein phosphatases in heart failure. A: Representative Western blots of LTCC, protein phosphatases and GAPDH from Sham and CAL rats. For each protein, the bands are taken from the same gel and have not been manipulated for contrast, color-balance, brightness or background. Solid lines demarcate the bands for the target protein and for

the GAPDH loading control, which were taken from the same gel. For each protein, the molecular weights of the bands are indicated. B: Mean band intensity expressed relative to Sham as 100%. Data are mean ± SEM from 3 Sham and 3 CAL hearts.

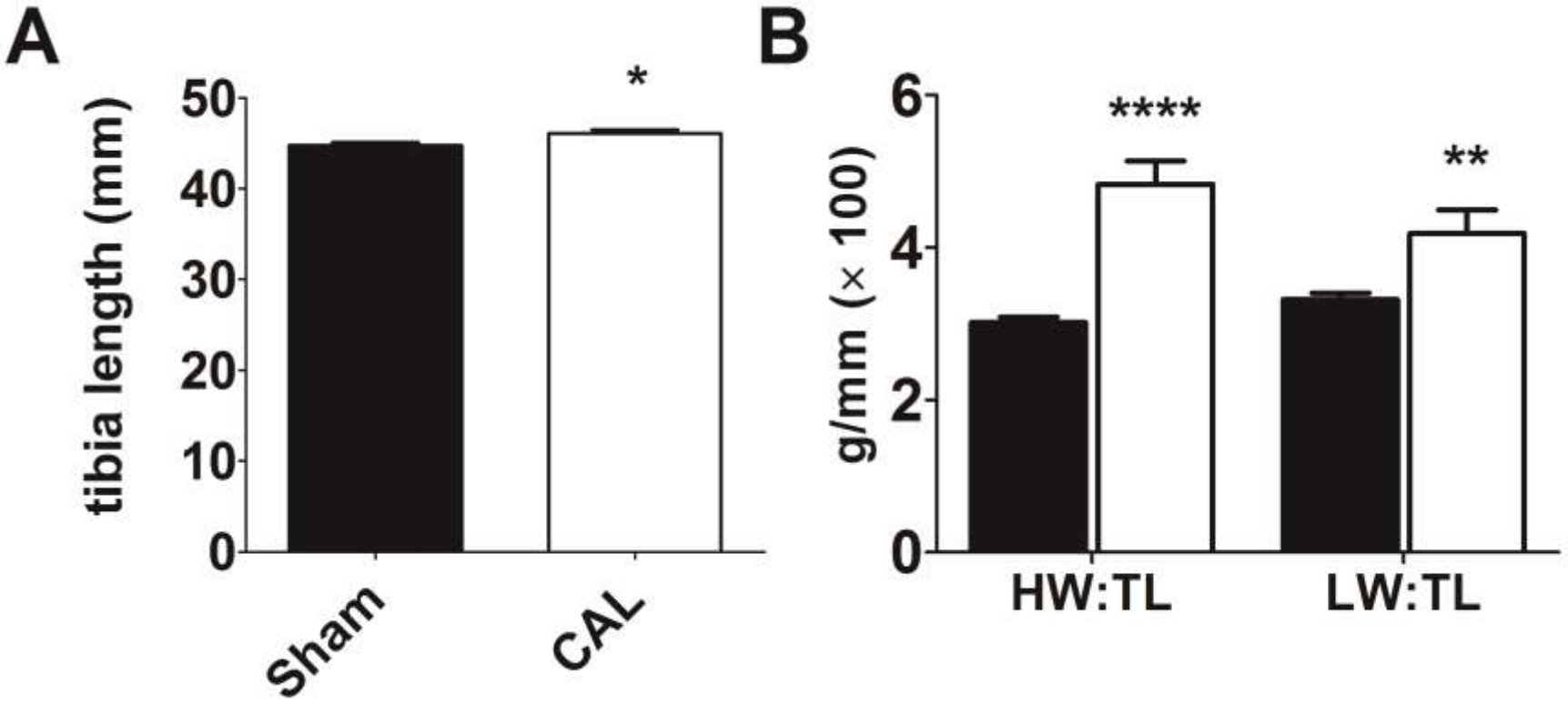
A
tibia length (mm)
50
40
30
20
10
0
*
Sham
CAL
B
g/mm (× 100)
6
4
2
0
****
**
HW:TL
LW:TL

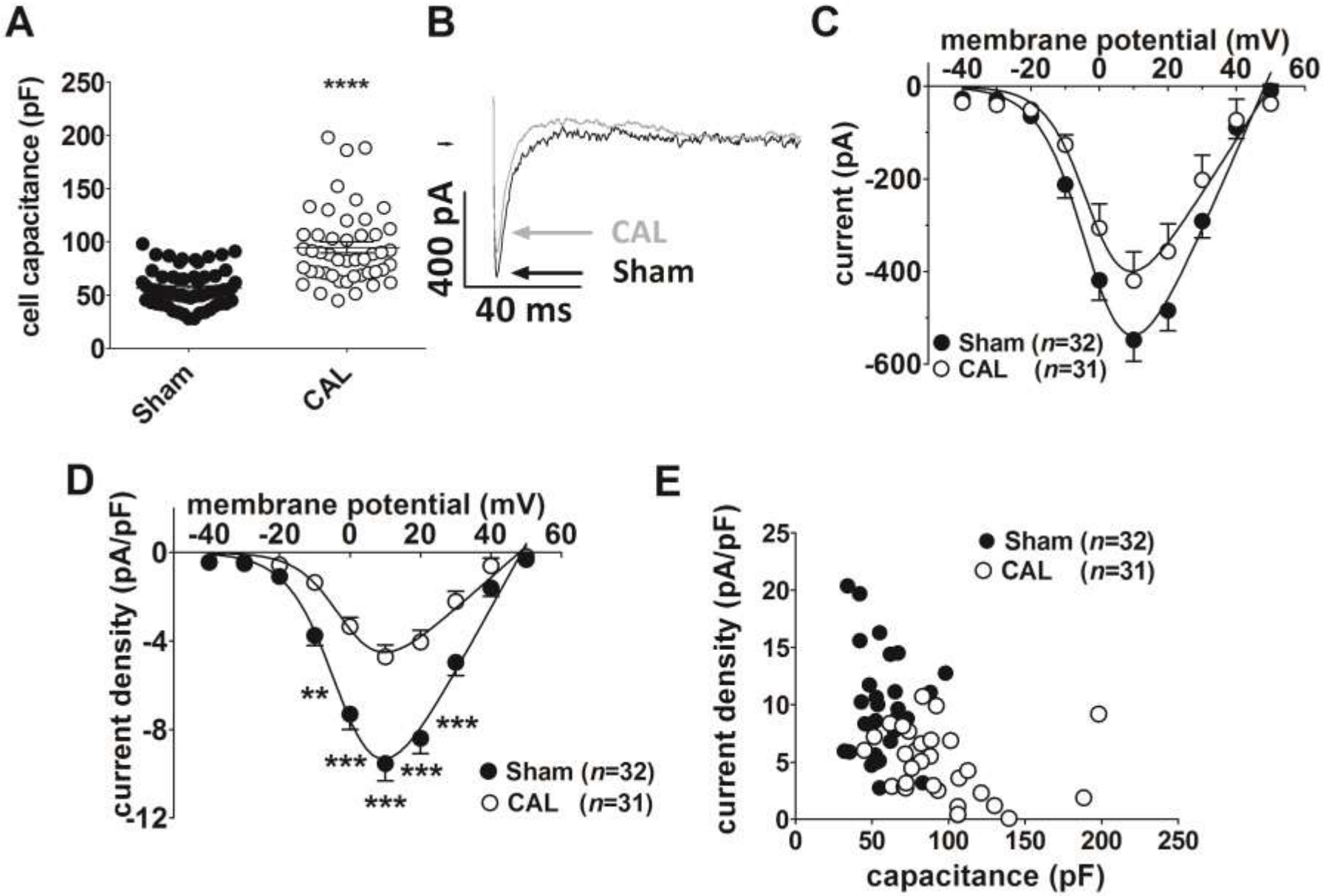
A
cell capacitance (pF)
250
200
150
100
50
0
****
Sham
CAL
B
400 pA
40 ms
CAL
Sham
C
membrane potential (mV)
-40
-20
0
20
40
60
current (pA)
0
-200
-400
-600
Sham (n=32)
CAL (n=31)
D
membrane potential (mV)
-40
-20
0
20
40
60
current density (pA/pF)
0
-4
-8
-12
**
***
***
***
***
Sham (n=32)
CAL (n=31)
E
current density (pA/pF)
25
20
15
10
5
0
0
50
100
150
200
250
capacitance (pF)
Sham (n=32)
CAL (n=31)

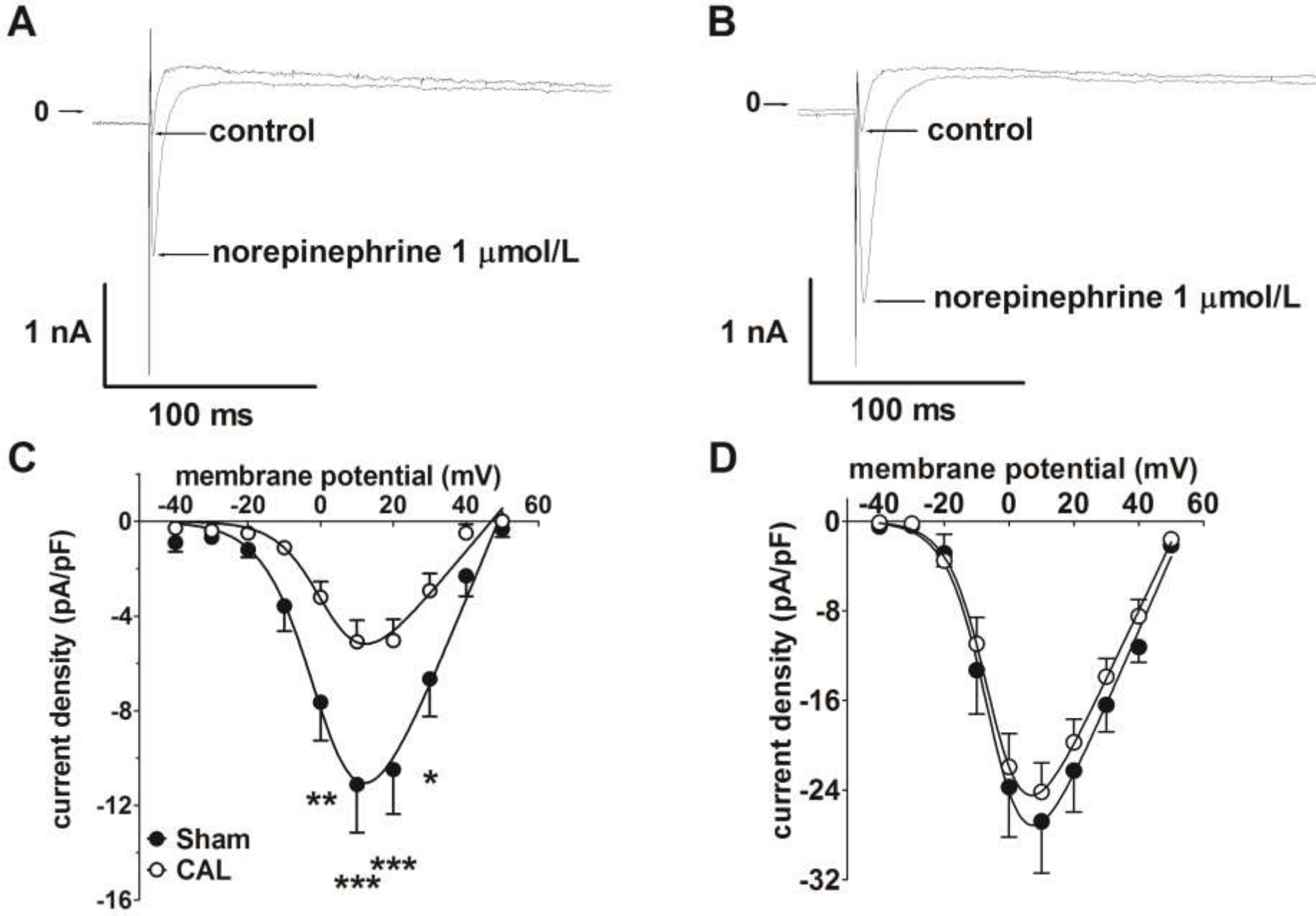
A
0
control
norepinephrine 1 μmol/L
1 nA
100 ms
B
0
control
norepinephrine 1 μmol/L
1 nA
100 ms
C
membrane potential (mV)
-40
-20
0
20
40
60
0
-4
-8
-12
-16
current density (pA/pF)
Sham
CAL
**
*
***
***
D
membrane potential (mV)
-40
-20
0
20
40
60
0
-8
-16
-24
-32
current density (pA/pF)

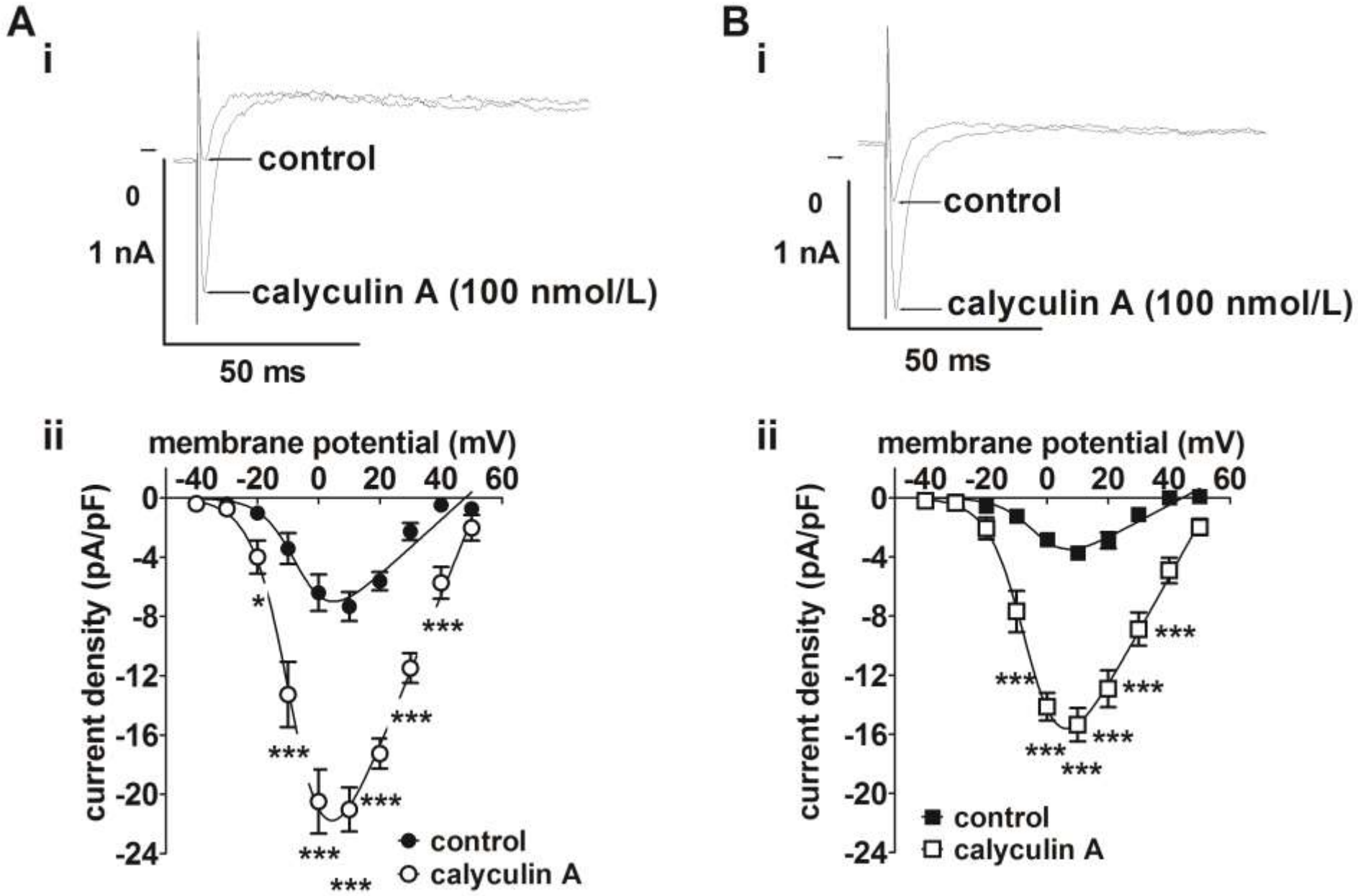
A
i
control
0
1 nA
calyculin A (100 nmol/L)
50 ms
ii
membrane potential (mV)
-40 -20 0 20 40 60
0
-4
-8
-12
-16
-20
-24
current density (pA/pF)
control
calyculin A
B
i
control
0
1 nA
calyculin A (100 nmol/L)
50 ms
ii
membrane potential (mV)
-40 -20 0 20 40 60
0
-4
-8
-12
-16
-20
-24
current density (pA/pF)
control
calyculin A

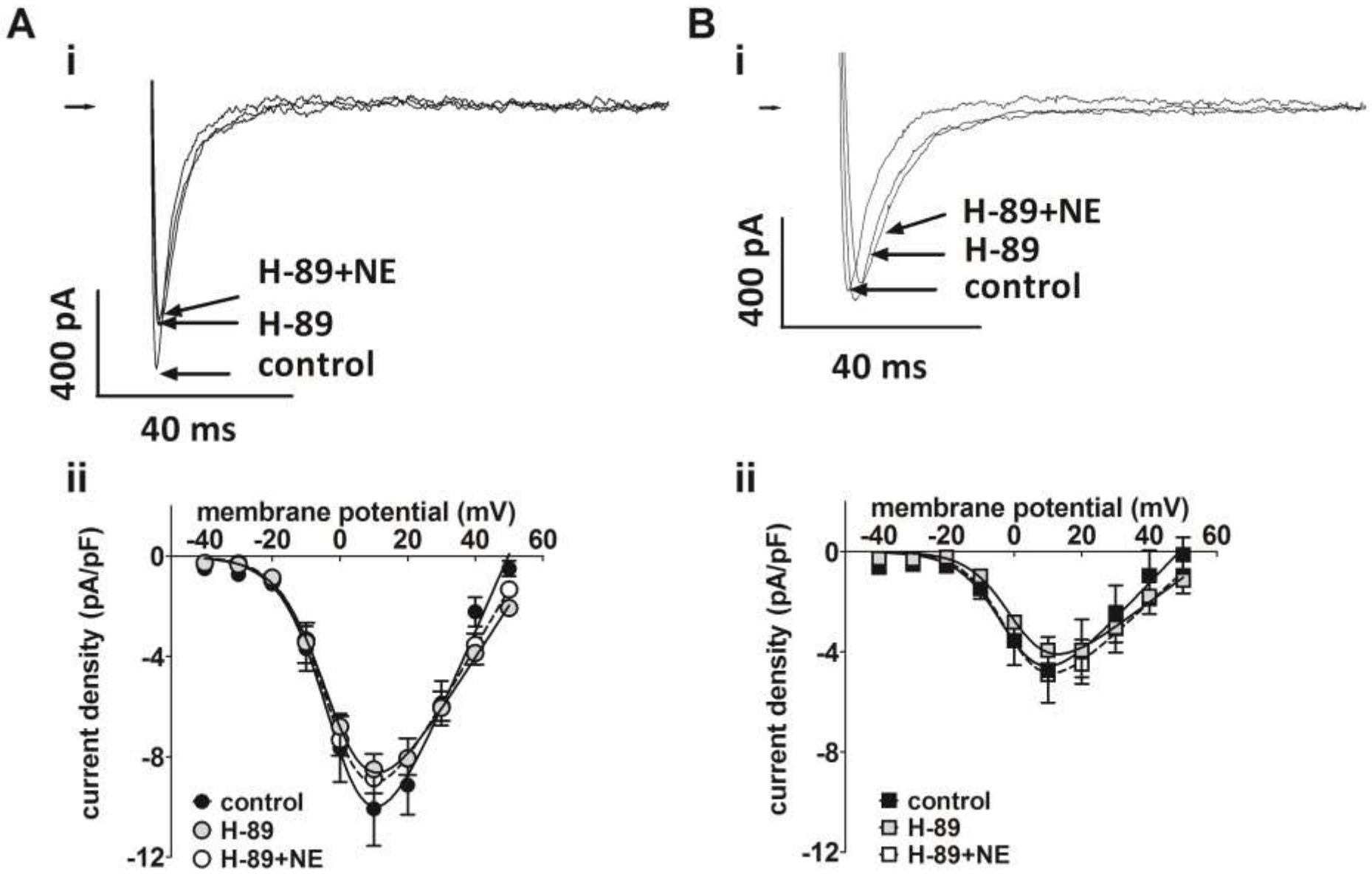
A
i
H-89+NE
H-89
control
400 pA
40 ms
ii
membrane potential (mV)
-40
-20
0
20
40
60
0
-4
-8
-12
current density (pA/pF)
control
H-89
H-89+NE
B
i
H-89+NE
H-89
control
400 pA
40 ms
ii
membrane potential (mV)
-40
-20
0
20
40
60
0
-4
-8
-12
current density (pA/pF)
control
H-89
H-89+NE

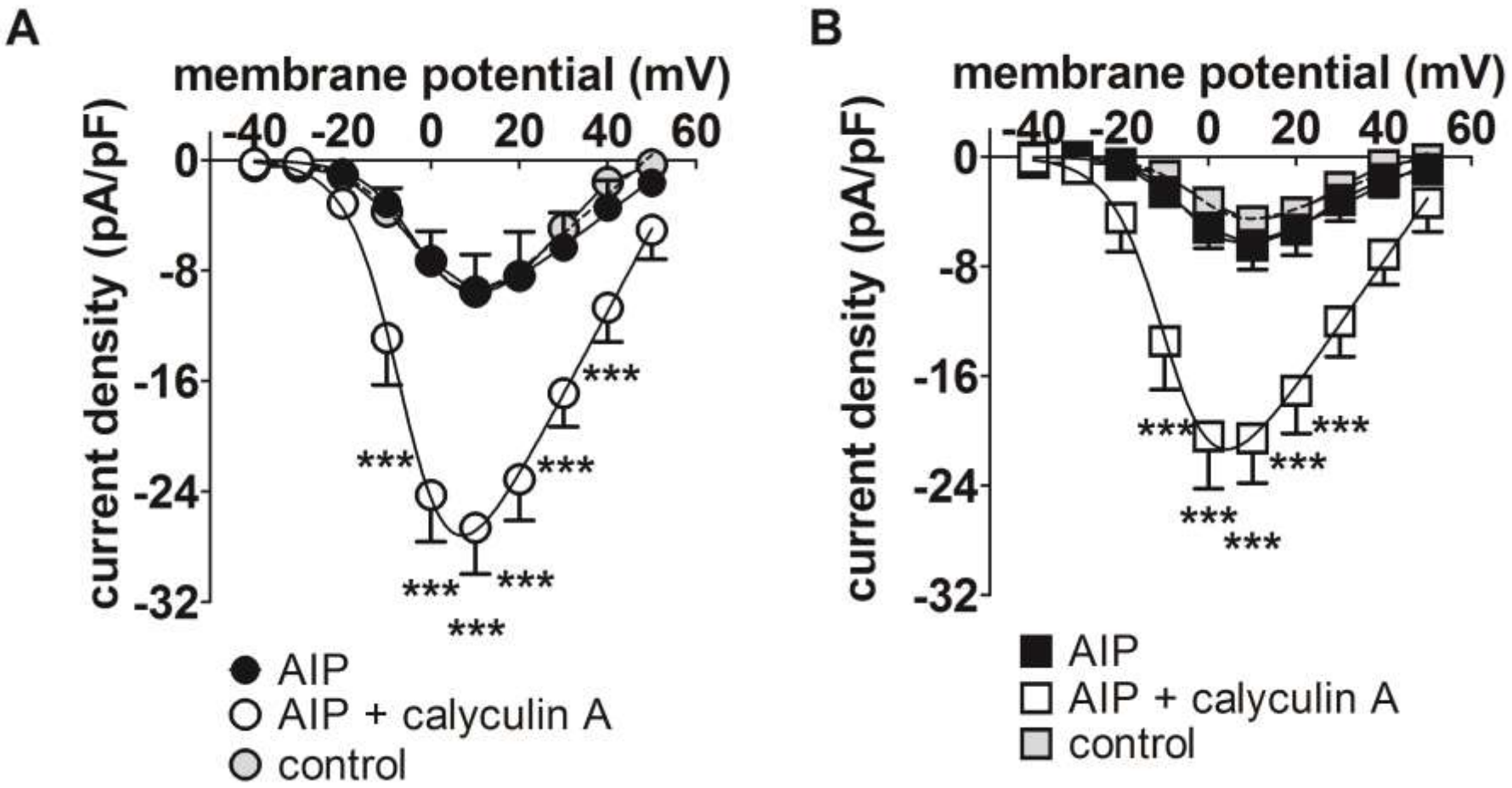
A
membrane potential (mV)
-40 -20 0 20 40 60
0
-8
-16
-24
-32
current density (pA/pF)
***
AIP
AIP + calyculin A
control
B
membrane potential (mV)
-40 -20 0 20 40 60
0
-8
-16
-24
-32
current density (pA/pF)
***
AIP
AIP + calyculin A
control

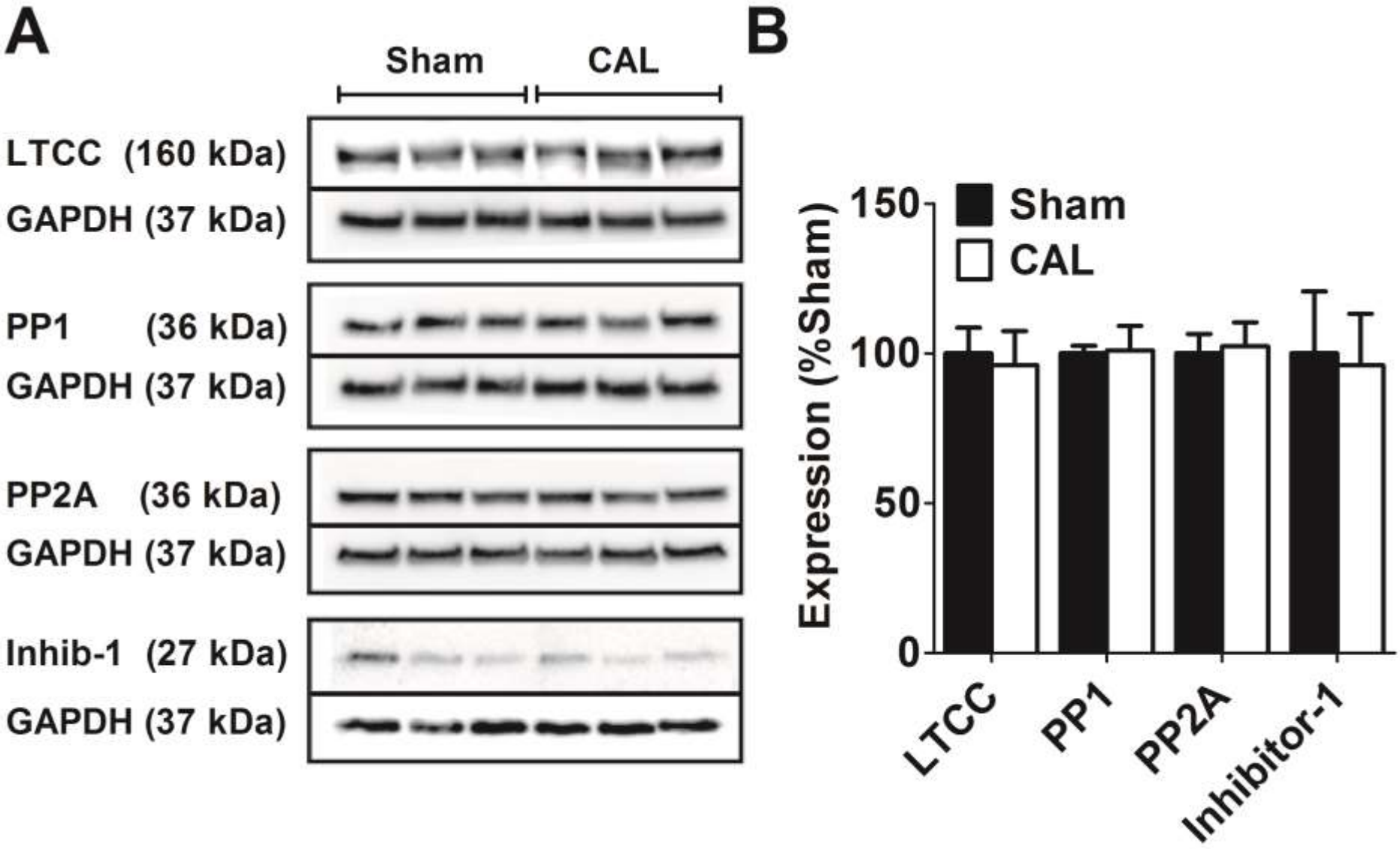
A
Sham
CAL
LTCC (160 kDa)
GAPDH (37 kDa)
PP1 (36 kDa)
GAPDH (37 kDa)
PP2A (36 kDa)
GAPDH (37 kDa)
Inhib-1 (27 kDa)
GAPDH (37 kDa)
B
Expression (%Sham)
150
100
50
0
Sham
CAL
LTCC
PP1
PP2A
Inhibitor-1